J|A|C|S
ARTICLES
Published on Web 02/12/2003

Porous Lanthanide-Organic Frameworks: Synthesis, Characterization, and Unprecedented Gas Adsorption Properties

Long Pan,[†,||] Kristie M. Adams,[†] Hayden E. Hernandez,[†] Xiaotai Wang,*[,†] Chong Zheng,[‡] Yoshiyuki Hattori,[§] and Katsumi Kaneko[§]

Contribution from the Department of Chemistry, University of Colorado at Denver, Campus Box 194, P.O. Box 173364, Denver, Colorado 80217-3364, Department of Chemistry and Biochemistry, Northern Illinois University, DeKalb, Illinois 60115, and Department of Chemistry, Faculty of Science, Chiba University, 1-33 Yayoi, Inage, Chiba 263-8522, Japan

Received October 17, 2002; E-mail: xwang@carbon.cudenver.edu

Abstract: The reactions of $Ln(NO_3)_3$ (Ln = La, Er) with 1,4-phenylendiacetic acid (H_2PDA) under hydrothermal conditions produce isostructural lanthanide coordination polymers with the empirical formula $[Ln_2(PDA)_3(H_2O)]\cdot 2H_2O$. The extended structure of $[Ln_2(PDA)_3(H_2O)]\cdot 2H_2O$ consists of Ln-COO triple helixes cross-linked through the $-CH_2C_6H_4CH_2-$ spacers of the PDA anions, showing 1D open channels along the crystallographic *c* axis that accommodate the guest and coordinated water molecules. Evacuation of $[Er_2(PDA)_3(H_2O)]\cdot 2H_2O$ at room temperature and at 200 °C, respectively, generates $[Er_2(PDA)_3(H_2O)]$ and $[Er_2(PDA)_3]$, both of which give powder X-ray diffraction patterns consistent with that of $[Er_2(PDA)_3(H_2O)]\cdot 2H_2O$. The porosity of $[Er_2(PDA)_3(H_2O)]$ and $[Er_2(PDA)_3]$ is further demonstrated by their ability to adsorb water vapor to form $[Er_2(PDA)_3(H_2O)]\cdot 2H_2O$ quantitatively. Thermogravimetric analyses show that $[Er_2(PDA)_3]$ remains stable up to 450 °C. The effective pore window size in $[Er_2(PDA)_3]$ is estimated at 3.4 Å. Gas adsorption measurements indicate that $[Er_2(PDA)_3]$ adsorbs CO_2 into its pores and shows nonporous behavior toward Ar or N_2. There is a general correlation between the pore size and the kinetic diameters of the adsorbates (CO_2 = 3.3 Å, Ar = 3.40 Å, and N_2 = 3.64 Å). That the adsorption favors CO_2 over Ar is unprecedented and may arise from the combined differentiations on size and on host−guest interactions.

Introduction

In recent years, the design and synthesis of metal-organic coordination polymers have attracted considerable attention,[1−5] for such supramolecular assemblies have interesting structures as well as potential applications as smart optoelectronic,[6,7] magnetic,[8] and porous materials.[9−11] A porous coordination polymer possesses a metal-organic framework with open channels where the guest species can be removed and reintroduced reversibly without collapse of the framework. Metal-organic frameworks derived from porous coordination polymers are of interest as heterogeneous catalysts, sensors, and storage and separation devices.

The past few years have seen impressive developments in using multitopic carboxylates as anionic ligands to support charge-neutral porous coordination networks.[12,13] Besides robustness, such networks exclude uncoordinated counterions that could occupy and block the open channels. These attributes are favored for porous applications such as size- and shape-selective separations and catalysis. Thus far, the assembly of metal-carboxylate networks has centered on d-block metal ions such as Zn(II), Cu(II), and Co(II), and the analogous chemistry of the lanthanide ions is still lacking in scope, although several research groups, ours included, have reported some interesting findings.[14−20] The coordination sites of such d-block metal ions

[†] University of Colorado at Denver.
[‡] Northern Illinois University.
[§] Chiba University.
[||] Current address: Department of Chemistry and Chemical Biology, Rutgers University, Piscataway, NJ 08854.

(1) Hollingsworth, M. D. *Science* **2002**, *295*, 2410.
(2) Moulton, B.; Zaworotko, M. J. *Chem. Rev.* **2001**, *101*, 1629.
(3) Eddaoudi, M.; Moler, D. B.; Li, H.; Chen, B.; Reineke, T. M.; O'Keeffe, M.; Yaghi, O. M. *Acc. Chem. Res.* **2001**, *34*, 319
(4) Robson, R. *J. Chem. Soc., Dalton Trans.* **2000**, 3735.
(5) Blake, A. J.; Champness, N. R.; Hubberstey, P.; Li, W.-S.; Withersby, M. A.; Schroder, M. *Coord. Chem. Rev.* **1999**, *183*, 117.
(6) Lin, W.; Wang, Z.; Ma, L. *J. Am. Chem. Soc.* **1999**, *121*, 11249.
(7) Evans, O. R.; Xiong, R.; Wang, Z.; Wong G. K.; Lin, W. *Angew. Chem., Int. Ed.* **1999**, *38*, 536.
(8) Kahn, O. *Acc. Chem. Res.* **2000**, *33*, 647.
(9) Eddaoudi, M.; Kim, J.; Rosi, N.; Vodak, D.; Wachter, J.; O'Keeffe, M.; Yaghi, O. M. *Science* **2002**, *295*, 469.
(10) Kuznicki, S. M.; Bell, V. A.; Nair, S.; Hillhouse, H. W.; Jacubinas, R. M.; Braunbath, C. M.; Toby, B. H.; Tspatsis, M. *Nature* **2001**, *412*, 720.
(11) Noro, S.; Kitazawa, S.; Kondo, M.; Seki, K. *Angew. Chem., Int. Ed.* **2000**, *39*, 2082.
(12) Eddaoudi, M.; Moler, D. B.; Li, H.; Chen, B.; Reineke, T. M.; O'Keeffe, M.; Yaghi, O. M. *Acc. Chem. Res.* **2001**, *34*, 319.
(13) Mori, W.; Takamizawa, S. *J. Solid State Chem.* **2000**, *152*, 120.
(14) Cao, R.; Sun, D.; Liang, Y.; Hong, M.; Tatsumi, K.; Shi, Q. *Inorg. Chem.* **2002**, *41*, 2087.
(15) Pan, L.; Zheng, N.; Wu, Y.; Han, S.; Yang, R.; Huang, X.; Li, J. *Inorg. Chem.* **2001**, *40*, 828.
(16) Reineke, T. M.; Eddaoudi, M.; O'Keeffe, M.; Yaghi, O. M. *Angew. Chem., Int. Ed.* **1999**, *38*, 2590.
(17) Reineke, T. M.; Eddaoudi, M.; Fehr, M.; Kelley, D.; Yaghi, O. M. *J. Am. Chem. Soc.* **1999**, *121*, 1651.
(18) Pan, L.; Woodlock, E. B.; Wang, X. *Inorg. Chem.* **2000**, *39*, 4174.
(19) Kiritsis, V.; Michaelides, A.; Skoulika, S.; Golhen, S.; Ouahab, L. *Inorg. Chem.* **1998**, *37*, 3407.

10.1021/ja028996w CCC: $25.00

are frequently occupied completely by the bridging carboxylates, leaving no accessible metal coordination sites in the network that might otherwise be utilized to carry out interesting chemistry such as catalysis. Because the lanthanide ions generally have higher coordination numbers than the d-block metal ions, incorporation of ancillary ligands (such as water molecules) into lanthanide coordination networks is made more likely. Such ancillary ligands may be removed without collapse of the lanthanide-organic framework, thereby generating porous solids with coordinatively unsaturated and Lewis-acidic lanthanide ions that have potential catalytic activity.[21,22] This rationale has led us and others to seek porous lanthanide carboxylates.

Among the reported network lanthanide carboxylates are those supported by rigid ring carboxylates such as 1,4-benzenedicarboxylate, and they have condensed structures containing no guest species.[15−17] In pursuit of porous lanthanide coordination polymers with less condensed and more open frameworks, we have chosen to use ring ligands with carboxylate groups connected to more flexible carbon atoms. We have reported an erbium(III) porous network of the formula $[Er(CTC)(H_2O)_2]\cdot 2.5H_2O$ (CTC = *cis*,*cis*-1,3,5-cyclohexanetricarboxylate trianion), where the coordinated (ancillary) and guest water molecules are shown inside and outside of the brackets, respectively.[18] Removal of the guest water generates the dehydrated solid $[Er(CTC)(H_2O)_2]$, which, despite losing long-range order, reverts to the original crystalline phase $[Er(CTC)(H_2O)_2]\cdot 2.5H_2O$ upon exposure to water vapor.

In this work, we present a study of lanthanide(III) coordination polymers supported by 1,4-phenylendiacetate, a readily available ligand material that heretofore has not been utilized to support metal-organic frameworks. These isostructural lanthanide(III) carboxylates, formulated empirically as $[Ln_2(PDA)_3(H_2O)]\cdot 2H_2O$ (Ln = La, Er; PDA = 1,4-phenylendiacetate dianion), have been synthesized through hydrothermolysis and structurally characterized via single-crystal X-ray diffraction. The erbium(III) compound $[Er_2(PDA)_3(H_2O)]\cdot 2H_2O$ has been used representatively in porosity studies, which led to the generation of well-defined porous phases $[Er_2(PDA)_3(H_2O)]$ and $[Er_2(PDA)_3]$ that exhibit novel and significant properties previously not observed for lanthanide-organic coordination polymers or other metal-organic frameworks.

Experimental Section

Materials and Methods. Lanthanum(III) and erbium(III) nitrates and 1,4-phenylendiacetic acid (H_2PDA) were purchased from commercial suppliers and were used without further purification. Infrared spectra (IR) were recorded on a Thermo-Nicolet Avatar 360 FTIR spectrometer from neat solids placed on the diamond window of a horizontal attenuated total reflectance accessory. Thermogravimetric (TG) analyses were performed under N_2 using a TA 2050 system. Powder X-ray diffraction (XRD) data were recorded on a Rigaku D/M-2200T automated diffractometer. Simulated XRD patterns were calculated with the SHELXTL-XPOW program using the single-crystal data. Microelemental analyses were performed by Atlantic Microlab in Norcross, GA. The adsorption isotherms were measured at 273 K for CO_2 and at 77 K for N_2 and Ar, using an Autosorb-1 system of Quantachrome and ultrapure gases (99.999%).

Synthesis of $[Ln_2(PDA)_3(H_2O)]\cdot 2H_2O$ (Ln = La, Er). Identical procedures were employed to prepare the two compounds; that for the erbium compound is described here in detail. A mixture of $Er(NO_3)_3\cdot 5H_2O$ (0.353 g, 0.80 mmol) and H_2PDA (0.095 g, 0.49 mmol) was placed in a Teflon-lined Parr bomb containing 10 mL of deionized water and 1 mL of ethanol. The bomb was sealed, heated at 170 °C for 3 days, and allowed to cool to room temperature. Pink crystals were isolated by decanting the supernatant, washed thoroughly with deionized water, ethanol, and acetone, and air-dried to give 0.124 g of product (78%). Main IR absorption bands (cm^{-1}): 3422 (w, br), 1529 (s, br), 1396 (s), 1278 (m), 718 (m). Anal. Calcd for $C_{30}H_{30}O_{15}Er_2$ = $[Er_2(PDA)_3(H_2O)]\cdot 2H_2O$: C, 37.34; H, 3.13. Found: C, 37.31; H, 3.00. The phase purity of the bulk products was checked by comparing its observed and simulated XRD patterns.

The lanthanum compound was prepared analogously using $Ln(NO_3)_3$. Main IR absorption bands (cm^{-1}): 3438 (w, br), 1523 (s, br), 1380 (s), 1270 (m), 711 (m). The phase purity of the bulk products was checked by comparing its observed and simulated XRD patterns.

Generation of $[Er_2(PDA)_3(H_2O)]$ and $[Er_2(PDA)_3]$. A freshly isolated sample of $[Er_2(PDA)_3(H_2O)]\cdot 2H_2O$ (218 mg) was evacuated under 2×10^{-3} Torr at room temperature for 4 h. The measured weight loss (8.0 mg) was equivalent to the loss of two water molecules per formula unit (calcd 8.1 mg). Another sample of $[Er_2(PDA)_3(H_2O)]\cdot 2H_2O$ (468 mg) was evacuated under 2×10^{-3} Torr at 200 °C for 4 h and allowed to cool to room temperature. The measured weight loss (26.0 mg) was equivalent to the loss of three water molecules per formula unit (calcd 26.2 mg). The XRD patterns of $[Er_2(PDA)_3(H_2O)]$ and $[Er_2(PDA)_3]$ are both consistent with that of $[Er_2(PDA)_3(H_2O)]\cdot 2H_2O$. Exposure of $[Er_2(PDA)_3(H_2O)]$ and $[Er_2(PDA)_3]$ to water vapor for 12 h resulted in weight gains corresponding to two and three water molecules per formula unit, respectively. The dehydration and rehydration processes were reversible.

Thermal Analyses. A TG analysis performed on a sample of $[Er_2(PDA)_3(H_2O)]\cdot 2H_2O$ showed continuous weight loss (5.47%) between 50 and 140 °C, which corresponded to the loss of three water molecules per formula unit (calcd 5.59%). No further weight loss was observed until it reached 450 °C, at which the decomposition of $[Er_2(PDA)_3]$ occurred, as indicated by a significant weight loss (57.1%). No attempt was made to identify the products of decomposition. A TG analysis of $[La_2(PDA)_3(H_2O)]\cdot 2H_2O$ gave similar results.

X-ray Crystallography. Several crystals of each compound were indexed on a Bruker SMART CCD diffractometer using 40 frames with an exposure time of 20 s per frame. One crystal of each compound with good reflection quality was chosen for data collection. The exposure time was 20 s for each frame. The reflections were collected in the hemisphere of the reciprocal lattice of the monoclinic cell to ensure enough redundancy. An empirical absorption correction using the program SADABS[23] was applied to all observed reflections. The structure was solved with direct methods using the SHELXTL program.[24] Full matrix least-squares refinement on F^2 was carried out using the SHELXTL program.[24] The unit cell information and refinement details are summarized in Table 1.

Results and Discussion

Syntheses and X-ray Structures. Coordination polymers of the formula $[Ln_2(PDA)_3(H_2O)]\cdot 2H_2O$ (Ln = La, Er; PDA = 1,4-phenylendiacetate dianion) were synthesized from the hydrothermal reactions of lanthanide(III) nitrates with 1,4-phenylendiacetic acid (H_2PDA). These crystalline solids are insoluble in water or common organic solvents such as acetone and

(20) Serpaggi, F.; Férey, G. *J. Mater. Chem.* **1998**, *8*, 2737.
(21) Shibasaki, M.; Yamada, K.-I.; Yoshikawa, N. Lanthanide Lewis Acids Catalysis. In *Lewis Acids in Organic Synthesis*; Yamamoto, H., Ed.; Wiley-VCH: New York, 1999; Vol. 2.
(22) Imamoto, T. *Lanthanide in Organic Synthesis*; Academic: New York, 1994.
(23) Sheldrick, G. M. SADABS. Program for Empirical Absorption Correction of Area Detector Data; University of Göttingen: Germany, 2002.
(24) Sheldrick, G. M. SHELXTL. Version 5.1; Bruker Analytical X-ray Systems Inc.: Madison, Wisconsin, 1997.

Table 1. Crystal Data and Structure Refinement for $[Ln_2(PDA)_3(H_2O)]\cdot 2H_2O$ (Ln = La, Er)

empirical formula	$[La_2(PDA)_3(H_2O)]\cdot 2H_2O$	$[Er_2(PDA)_3(H_2O)]\cdot 2H_2O$
formula weight	908.36	965.06
crystal system	monoclinic	monoclinic
space group	$P2_1/c$ (No. 14)	$P2_1/c$ (No. 14)
a (Å)	22.101(7)	21.6200(2)
b (Å)	10.218(3)	9.97190(10)
c (Å)	14.283(5)	14.04530(10)
β (°)	91.276(6)	91.5840(10)
V (Å^3)	3224.8(18)	3026.90(5)
Z	4	4
T (K)	293(2)	293(2)
d_{calcd} (g/cm^3)	1.871	2.118
λ (Mo Kα) (Å)	0.71073	0.71073
μ (mm^{-1})	2.686	5.583
data/restraints/ parameters	4621/0/448	7172/0/425
final R indices[a]		
[$I > 2\sigma I$)]		
R1	0.0530	0.0643
wR2	0.1278	0.1010
R indices (all data)		
R1	0.0571	0.0797
wR2	0.1304	0.1052

[a] $R1 = \sum||F_o| - |F_c||/\sum|F_o|$; $wR2 = [\sum[w(F_o^2 - F_c^2)^2]/\sum[w(F_o^2)^2]]^{1/2}$.

ethanol. The IR spectra of the two compounds are similar, each showing strong absorption bands between 1350 and 1550 cm^{-1} that are diagnostic of coordinated carboxylate groups.[25] The absence of the strong carboxyl absorption band at 1698 cm^{-1} for H_2PDA indicates complete deprotonation of H_2PDA. Single-crystal X-ray diffraction analyses revealed that the two compounds are isostructural, and the structure of $[Er_2(PDA)_3(H_2O)]\cdot 2H_2O$ is described here representatively. The numbers of crystallographically independent Er(III) cations and PDA anions are two and four, respectively. Figure 1 shows the metal coordination environment in $[Er_2(PDA)_3(H_2O)]\cdot 2H_2O$. While both Er(III) ions are coordinated by eight oxygen atoms from six COO^- groups of different PDA anions, only one (Er1) is additionally coordinated by a water molecule. The coordination geometry around Er1 may be described as a tricapped trigonal prism, with O21, O41, O23, O32#1, O11, and O13#1 filling the vertexes and O12, O24, and OW1 capping the rectangular faces. The coordination geometry for eight-coordinate Er2 is close to that of a dodecahedron. The Er−O (carboxylate) bond distances range from 2.239(7) to 2.677(8) Å, and that of the Er−O (aqua) bond is 2.367(7) Å, all of which are within the range of those observed for other eight- or nine-coordinate Er(III) complexes with oxygen donor ligands.[18,26] Selected bond distances and angles are presented in Table 2.

In the polymeric structure of $[Er_2(PDA)_3(H_2O)]\cdot 2H_2O$, the Er(III) ions are interconnected through COO^- groups, forming what may be viewed as an Er-COO triple helix that extends in the crystallographic c direction (Figure 2). The two types of Er(III) ions, which adopt an extended zigzag orientation, act as nodes alternately, and three COO^- groups bridge two adjacent Er(III) ions in bis-monodentate syn−syn (e.g., −O21−C28−O22−) and tridentate (e.g., −O11−C18−O12−) bonding modes. These one-dimensional (1D) infinite helixes may be viewed as supramolecular SBUs (secondary building blocks) that are further cross-linked via the $-CH_2C_6H_4CH_2-$ spacers

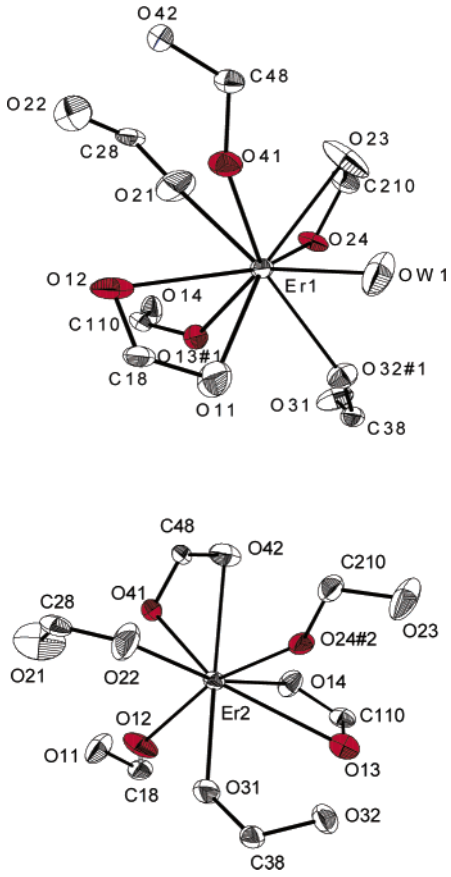

Figure 1. ORTEP diagrams showing the coordination environment for Er1 (top) and Er2 (bottom) in $[Er_2(PDA)_3(H_2O)]\cdot 2H_2O$. Thermal ellipsoids are at 30% probability. Oxygen atoms in red are coordinated to both Er1 and Er2. Symmetry labels #1 and #2 are specified in Table 2.

Chart 1

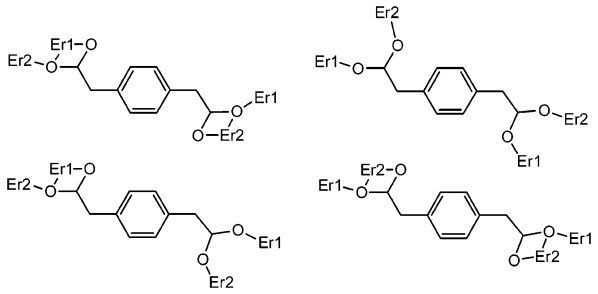

of the PDA anions (Chart 1). Viewed along the crystallographic c axis, the resulting 3D network of $[Er_2(PDA)_3(H_2O)]\cdot 2H_2O$ is reminiscent of the shape of a compressed honeycomb, showing 1D open channels (Figure 3). The guest water molecules suspend in the channels, and the coordinated water molecules point away from the Er-PDA framework and into the channels.

Dehydration and Porosity. The openness of the channels makes it possible to remove the guest and coordinated water molecules from $[Er_2(PDA)_3(H_2O)]\cdot 2H_2O$. Evacuation of $[Er_2(PDA)_3(H_2O)]\cdot 2H_2O$ at room temperature removed the guest water molecules quantitatively, affording the dehydrated solid $[Er_2(PDA)_3(H_2O)]$, whose XRD pattern is consistent with that of $[Er_2(PDA)_3(H_2O)]\cdot 2H_2O$ (Figure 4). This indicates preservation of the framework and retention of the crystalline order upon removal of the guest species; the latter property has had only a few precedents in lanthanide coordination polymers.[27,28] Further removal of the coordinated water ligand could maximize pore

(25) Nakamoto, K. *Infrared and Raman Spectra of Inorganic and Coordination Compounds*, 5th ed.; Wiley & Sons: New York, 1997.
(26) Sugita, Y.; Ouchi, A. *Bull. Chem. Soc. Jpn.* **1987**, *60*, 171.

Table 2. Selected Bond Distances and Angles for $[Er_2(PDA)_3(H_2O)]\cdot 2H_2O$[a]

Er(1)−O(24)	2.444(6)	Er(2)−O(24#2)	2.267(6)
Er(1)−O(23)	2.434(7)	Er(2)−O(42)	2.336(6)
Er(1)−O(41)	2.372(6)	Er(2)−O(41)	2.530(7)
Er(1)−O(21)	2.291(8)	Er(2)−O(22)	2.285(7)
Er(1)−O(12)	2.677(8)	Er(2)−O(12)	2.268(7)
Er(1)−O(13#1)	2.380(7)	Er(2)−O(31)	2.239(7)
Er(1)−O(11)	2.384(7)	Er(2)−O(13)	2.635(7)
Er(1)−O(32#1)	2.315(6)	Er(2)−O(14)	2.375(6)
Er(1)−OW1	2.367(7)		

O(24)−Er(1)−O(23)	52.3(2)	O(13#1)−Er(1)−OW1	144.7(2)
O(24)−Er(1)−O(41)	125.3(2)	O(11)−Er(1)−O(32#1)	75.4(2)
O(24)−Er(1)−O(21)	74.5(3)	O(11)−Er(1)−OW1	78.7(3)
O(24)−Er(1)−O(12)	141.3(2)	O(32#1)−Er(1)−OW1	70.8(2)
O(24)−Er(1)−O(13#1)	69.9(2)	O(24#1)−Er(2)−O(42)	79.1(2)
O(24)−Er(1)−O(11)	145.5(2)	O(24#1)−Er(2)−O(41)	131.3(2)
O(24)−Er(1)−O(32#1)	75.3(2)	O(24#1)−Er(2)−O(22)	78.1(3)
O(24)−Er(1)−OW1	108.2(3)	O(24#1)−Er(2)−O(12)	161.7(2)
O(23)−Er(1)−O(41)	78.2(2)	O(24#1)−Er(2)−O(31)	82.0(2)
O(23)−Er(1)−O(21)	77.8(3)	O(24#1)−Er(2)−O(13)	68.2(2)
O(23)−Er(1)−O(12)	136.4(3)	O(24#1)−Er(2)−O(14)	101.0(2)
O(23)−Er(1)−O(13#1)	120.0(2)	O(42)−Er(2)−O(41)	52.3(2)
O(23)−Er(1)−O(11)	153.7(3)	O(42)−Er(2)−O(22)	84.4(3)
O(23)−Er(1)−O(32#1)	101.9(3)	O(42)−Er(2)−O(12)	119.1(3)
O(23)−Er(1)−OW1	75.8(3)	O(42)−Er(2)−O(31)	156.9(3)
O(41)−Er(1)−O(21)	73.6(3)	O(42)−Er(2)−O(13)	110.8(2)
O(41)−Er(1)−O(12)	63.0(2)	O(42)−Er(2)−O(14)	80.6(3)
O(41)−Er(1)−O(13#1)	89.2(3)	O(41)−Er(2)−O(22)	92.6(3)
O(41)−Er(1)−O(11)	89.2(3)	O(41)−Er(2)−O(12)	66.8(2)
O(41)−Er(1)−O(32#1)	144.9(2)	O(41)−Er(2)−O(31)	143.5(2)
O(41)−Er(1)−OW1	75.4(3)	O(41)−Er(2)−O(13)	127.5(2)
O(21)−Er(1)−O(12)	73.0(3)	O(41)−Er(2)−O(14)	76.5(2)
O(21)−Er(1)−O(13#1)	72.3(3)	O(22)−Er(2)−O(12)	100.2(3)
O(21)−Er(1)−O(11)	121.0(3)	O(22)−Er(2)−O(31)	78.8(3)
O(21)−Er(1)−O(32)	141.3(3)	O(22)−Er(2)−O(13)	138.7(3)
O(21)−Er(1)−OW1	142.5(3)	O(22)−Er(2)−O(14)	164.8(3)
O(12)−Er(1)−O(13)	80.7(2)	O(12)−Er(2)−O(31)	79.8(3)
O(12)−Er(1)−O(11)	49.5(2)	O(12)−Er(2)−O(13)	104.4(2)
O(12)−Er(1)−O(32)	121.2(2)	O(12)−Er(2)−O(14)	85.4(3)
O(12)−Er(1)−OW1	110.3(3)	O(31)−Er(2)−O(13)	73.6(2)
O(13)−Er(1)−O(11)	85.1(3)	O(31)−Er(2)−O(14)	116.3(3)
O(13)−Er(1)−O(32)	74.9(2)	O(13)−Er(2)−O(14)	51.0(2)

[a] Symmetry transformations used to generate equivalent atoms: #1, x, $-y+{}^3/_2$, $z+{}^1/_2$; #2, x, $-y+{}^3/_2$, $z-{}^1/_2$.

volume and achieve a porous metal-organic framework with coordinatively unsaturated and Lewis-acidic lanthanide ions. Assisted by TG measurements, a preparative-scale sample of $[Er_2(PDA)_3(H_2O)]\cdot 2H_2O$ was heated at 200 °C under vacuum, causing the loss of three water molecules per formula unit. The resulting solid $[Er_2(PDA)_3]$ retains the framework and crystallinity observed in the original compound $[Er_2(PDA)_3(H_2O)]\cdot 2H_2O$, as supported by the consistent XRD patterns of the two substances (Figure 4). Previously, there have been reports of lanthanide-organic frameworks derived from removing ancillary ligands.[15−19] Such materials typically show loss of crystalline order and/or collapse or distortion of framework, as compared with the original coordination polymers. $[Er_2(PDA)_3]$ represents a rare example of a crystalline and structurally well-defined lanthanide-organic framework with ancillary ligands totally removed and Lewis-acidic metal sites opened up. Furthermore, according to TG analyses, $[Er_2(PDA)_3]$ remains stable up to 450 °C at which it begins to decompose. The structural stability of $[Er_2(PDA)_3]$ could be in part due to eight-coordination around

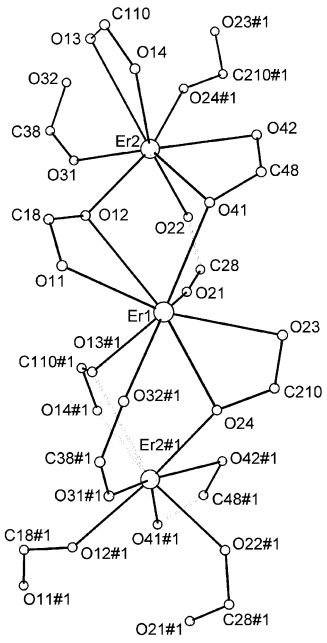

Figure 2. Fragment of the Er-COO helix. The aqua ligand on Er1 is omitted.

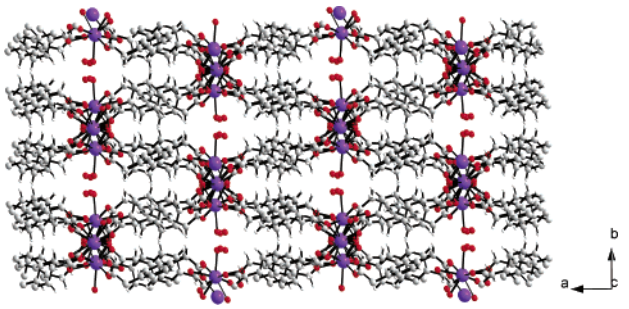

Figure 3. Representation of the extended structure of $[Er_2(PDA)_3(H_2O)]\cdot 2H_2O$. Color scheme: Er, blue; O, red; C, gray; H, white. H atoms in H_2O molecules are omitted.

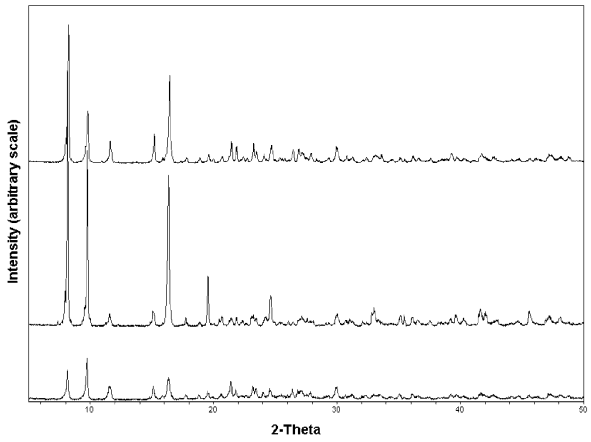

Figure 4. XRD patterns: $[Er_2(PDA)_3(H_2O)]\cdot 2H_2O$ (top), $[Er_2(PDA)_3(H_2O)]$ (middle), and $[Er_2(PDA)_3]$ (bottom).

each Er(III) ion. This observation dovetails with an earlier comment that while removal of both coordinated water molecules from $[Er(CTC)(H_2O)_2]$ leads to framework collapse, the Er-CTC framework is retained in $[Er(CTC)(H_2O)]$ where each Er(III) ion is still eight-coordinate.[18] One additional reason could be that the carboxylate groups in $[Er_2(PDA)_3]$ all act in the bridging mode and most of them also act in the chelating mode.

(27) Serpaggi, F.; Luxbacher, T.; Cheetham, A. K.; Férey, G. *J. Solid State Chem.* **1999**, *145*, 580.
(28) Dimos, A.; Tsaousis, D.; Michaelides, A.; Skoulika, S.; Golhen, S.; Ouahab, L.; Didierjean, C.; Aubry, A. *Chem. Mater.* **2002**, *14*, 2616.

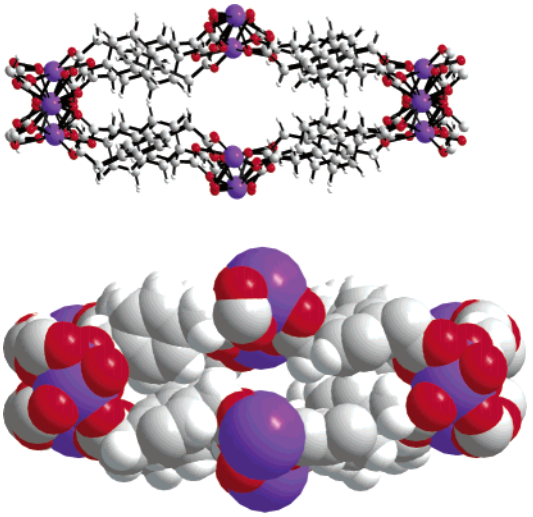

Figure 5. Cross section of the open channel in $[Er(PDA)_{1.5}]$: ball-and-stick model (top), space-filling model (bottom). Color scheme: Er, blue; O, red; C, gray; H, white.

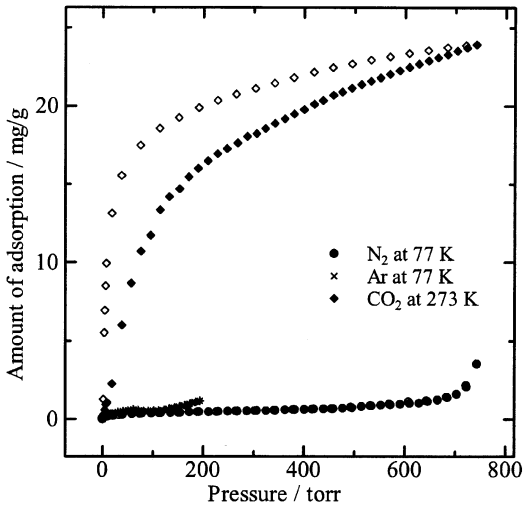

Figure 6. Adsorption isotherms of CO_2, N_2, and Ar. ◆ and ◇ represent adsorption and desorption of CO_2, respectively. Saturation vapor pressures: $P_o(CO_2) = 2.7 \times 10^4$ Torr (273 K), $P_o(Ar) = 200$ Torr (77 K), and $P_o(N_2) = 760$ Torr (77 K).

The porous nature of $[Er_2(PDA)_3(H_2O)]$ and $[Er_2(PDA)_3]$ was further demonstrated by their ability to adsorb water vapor to form $[Er_2(PDA)_3(H_2O)]\cdot 2H_2O$. The dehydration and rehydration processes were reversible.

The well-defined structure of $[Er_2(PDA)_3]$ allows us to estimate its pore window size by computationally removing the guest and coordinated water molecules from the crystal structure of $[Er_2(PDA)_3(H_2O)]\cdot 2H_2O$. While a ball-and-stick model reveals three localized openings on the cross section of the open channel, a space-filling model suggests that only the middle aperture, which shows an approximately circular contour, has an effective dimension (ca. 3.4 Å) that is large enough for uptake of adsorbates (Figure 5).[29]

Adsorption Phenomena. There have appeared in the literature reports of adsorption behavior of porous metal-organic frameworks derived from coordination polymers.[30−36] On the basis of careful studies, Rosseinsky et al. recently have made two observations on some metal-organic framework adsorbents: (1) the adsorbents may not be well-defined structurally, and (2) the actual porous structures responsible for uptaking the adsorbates may result from the adsorbents undergoing guest-directed framework transformations.[37] Such adsorbent characteristics are different from those of zeolites to which the adsorbents are frequently compared, for zeolites have known framework structures that are largely insensitive to uptake of guest species.[38] Thus, there are many open questions with respect to the adsorption behavior of metal-organic frameworks. The well-defined porous framework $[Er_2(PDA)_3]$ makes a good system for adsorption studies. Samples of $[Er(PDA)_{1.5}]$ were subjected to gas adsorption measurements using CO_2, Ar, and N_2, whose kinetic diameters are known to be 3.3, 3.40, and 3.64 Å, respectively.[38] It was observed that $[Er_2(PDA)_3]$ adsorbs CO_2 into its pores and shows nonporous behavior toward Ar or N_2 (Figure 6), which indicates a general correlation between the pore size and the kinetic diameters of the adsorbates.[39] N_2 cannot be adsorbed apparently because its kinetic diameter is greater than the effective pore window size. $[Er_2(PDA)_3]$ favors CO_2 over Ar in porous adsorption, despite the subtle difference (0.1 Å) in the kinetic diameters of the two gases. Such selectivity is unprecedented for porous metal-organic frameworks and may arise from the combined differentiations on size and on host−guest interactions. The framework host, which contains Er(III) ions, polar groups, and π-electrons, gives rise to an electric field that induces a dipole in CO_2. Besides such dipole−induced-dipole interactions, the quadrupole moment of CO_2 would interact with the electric field gradient, making a further contribution to the potential energy of adsorption.[40] In addition, there may be some donor−acceptor affinity between the Lewis-acidic Er(III) ions and the CO_2 molecules. In the case of Ar, the only major interactions are dipole−induced-dipole forces.

The steep rise in the adsorption branch of CO_2 was observed at extremely low pressures relative to the saturation vapor pressure of CO_2, and this high initial uptake indicates the presence of intrinsic micropores in $[Er_2(PDA)_3]$. Calculations based on the Dubinin−Radushkevitch (DR) equation gave a pore volume of $[Er_2(PDA)_3]$ (0.027 mL/g), as well as an isosteric heat of adsorption of CO_2 at 273 K (30.1 kJ/mol).[41,42] The relatively small pore volume can be understood with reference to the extended structure of $[Er_2(PDA)_3(H_2O)]\cdot 2H_2O$ that has no additional open channels along the *a* and *b* axes. The heat of adsorption is somewhat larger than that (20 kJ/mol) determined for CO_2 in silicalite-I,[43] probably because of the

(29) The La analogue has the same porous structure with essentially equivalent pore sizes.
(30) Kitaura, R.; Fujimoto, K.; Noro, S.-i.; Kondo, M.; Kitagawa, S. *Angew. Chem., Int. Ed.* **2002**, *41*, 133.
(31) Seki, K.; *Phys. Chem. Chem. Phys.* **2002**, *4*, 1968.
(32) Li, D.; Kaneko, K. *Chem. Phys. Lett.* **2001**, *335*, 50.
(33) Edgar, M.; Mitchell, R.; Slawin, A. M. Z.; Lightfoot, P.; Wright, P. A. *Chem.-Eur. J.* **2001**, *7*, 5168.
(34) Fletcher, A. J.; Cussen, E. J.; Prior, T. J.; Rosseinsky, M. J.; Kepert, C. J.; Thomas, K. M. *J. Am. Chem. Soc.* **2001**, *123*, 10001.
(35) Li, D.; Kaneko, K. *J. Phys. Chem. B* **2000**, *104*, 8940.
(36) Eddaoudi, M.; Li, H.; Yaghi, O. M. *J. Am. Chem. Soc.* **2000**, *122*, 1391.
(37) Cussen, E. J.; Claridge, J. B.; Rosseinsky, M. J.; Kepert, C. J. *J. Am. Chem. Soc.* **2002**, *124*, 9574.
(38) Breck, D. W. *Zeolite Molecular Sieves*; Wiley & Sons: New York, 1974.
(39) The adsorption isotherms of Ar and N_2 measured at 300 K also suggest nonporous behavior of $[Er_2(PDA)_3]$ toward these adsorbates.
(40) Gregg, S. J.; Sing, K. S. W. *Adsorption, Surface Area and Porosity*; Academic Press: New York, 1982.
(41) Dubinin, M. M. *Carbon* **1989**, *27*, 457.
(42) Stoeckli, H. F. In *Porosity in Carbons: Characterization and Applications*; Patrick, J. W., Ed.; Halsted: New York, 1995; Chapter 3.
(43) Choudhary, V. R.; Mayadevi, S. *Zeolites* **1996**, *17*, 501.

comparatively stronger host−guest interactions as described above. However, the heat of adsorption is still far smaller than those typical of chemical adsorption. For example, the heats of chemisorption of CO in Co and of CO_2 in Ni are 176 and 184 kJ/mol, respectively.[44] Thus, the nature of the $[Er_2(PDA)_3]$−CO_2 interaction is mainly physisorption without significant chemical association. Another interesting feature of the CO_2 isotherm is the hysteresis loop between the adsorption and desorption branches, which makes the isotherm different from types I−V in the IUPAC classification scheme.[40] The mechanism for hysteresis in the adsorption/desorption isotherms of metal-organic frameworks is not well understood currently; however, guest-directed framework rearrangements have been proposed for some labile metal-polypyridine networks.[30,37] It is unlikely that this mechanism operates in the hysteresis described here, for $[Er_2(PDA)_3]$ has a stable framework. Most likely, the hysteresis results from the hindered diffusion of CO_2 molecules in the pores of $[Er_2(PDA)_3]$, for the kinetic diameter of CO_2 is extremely close to the effective pore dimension.

Conclusions

We have synthesized novel isostructural lanthanide coordination polymers of the formula $[Ln_2(PDA)_3(H_2O)]\cdot 2H_2O$. We have used $[Er_2(PDA)_3(H_2O)]\cdot 2H_2O$ representatively to investigate the porous behavior of such compounds. Both the guest and the coordinated water molecules can be removed from the open channels of $[Er_2(PDA)_3(H_2O)]\cdot 2H_2O$, yielding $[Er_2(PDA)_3(H_2O)]$ and $[Er_2(PDA)_3]$, respectively. Both of these porous phases maintain the framework and crystalline order found in the original compound $[Er_2(PDA)_3(H_2O)]\cdot 2H_2O$, as shown by XRD analyses. The framework polymer $[Er_2(PDA)_3]$ is highly robust, remaining stable up to 450 °C. $[Er_2(PDA)_3]$ adsorbs CO_2, but not Ar or N_2, apparently because of size selectivity and the nature of host−guest interactions. Taken together, the results presented in this work illustrate the structure−property relationship at the supramolecular level. They also demonstrate the feasibility of achieving well-defined porous and stable lanthanide-organic frameworks with coordinatively unsaturated metal sites. Currently, we are extending this work to larger spacer ligands, hoping to attain lanthanide-organic frameworks with Lewis-acidic lanthanide ions arrayed on the wall of large open channels. Such systems would be well suited for the study of size- and shape-selective catalysis of various important organic reactions known to be catalyzed by lanthanide Lewis acids.[21,22]

Acknowledgment. We acknowledge support for this work from the University of Colorado at Denver; Research Corporation; and the donors of the Petroleum Research Fund, administered by the American Chemical Society. We thank Dr. Jing Li for XRD instrumentation assistance and Drs. Victor S. Lin, Mietek Jaroniec, Ping Liu, and Youchang Xie for helpful discussions. We also thank the reviewers for their suggestions and comments.

Supporting Information Available: Complete X-ray crystallographic files in CIF format. This material is available free of charge via the Internet at http://pubs.acs.org.

JA028996W

(44) Hayward, D. O.; Trapnell, B. M. W. *Chemisorption*, 2nd ed.; Butterworth: Washington, 1964.